Materials and methods

Subjects

We analyzed genotypes in DNA samples from 319 healthy postmenopausal Japanese women (66.7 ± 8.9 years, mean ± SD). We excluded women having endocrine disorders such as hyperthyroidism, hyperparathyroidism, diabetes mellitus, liver disease, and renal disease; those who used medications known to affect bone metabolism (e.g., corticosteroids, anticonvulsants, and heparin); and those with an unusual gynecologic history. All subjects were unrelated volunteers. Each subject was provided informed consent before entering the study.

Measurement of bone mineral density and biochemical markers

We measured the lumbar spine BMD and total body BMD of participants by dual-energy X-ray absorptiometry using the fast-scan mode (DPX-L; Lunar, Madison, WI). The BMD data were recorded as Z scores, as the deviation from the weight-adjusted average BMD for each year of age, based on data from 20,000 Japanese women. We also measured subjects' serum concentrations of alkaline phosphatase (ALP), intact osteocalcin (I-OC), intact parathyroid hormone (PTH), calcitonin, 1,25 $(OH)_2D_3$, total cholesterol (TC) and triglyceride(TG). We also measured urinary ratios of deoxypyridinoline (DPD) to creatinine using the HPLC method.

Determination of a single nucleotide polymorphism in the ALOX15 gene

We extracted a polymorphic variation of the putative *ALOX15* gene promoter/enhancer region from the Assays-on-Demand™ SNP Genotyping Products database (Applied Biosystems, Foster City, CA) and, according to its localization on the gene, denoted it -5299 G>A. We determined the –5299G/A polymorphism of the *ALOX15* gene using the TaqMan (Applied Biosystems) polymerase chain reaction (PCR) method [24]. To determine the *ALOX15* SNP we used Assays-on-Demand SNP Genotyping Products C_926671_10 (Applied BioSystems), which contains sequence-specific forward and reverse primers and two TaqMan MGB probes for detecting alleles. During the PCR cycle, two TaqMan probes competitively hybridize to a specific sequence of the target DNA and the reporter dye is separated from the quencher dye, resulting in an increase in fluorescence of the reporter dye. The fluorescence levels of the PCR products were measured with the ABI PRISM 7000 (Applied Biosystems), resulting in clear identification of three genotypes of the SNP.

Statistical analysis

We divided subjects into those having one or two chromosomes of the major A-allele and those with only the minor G-allele encoded at the same locus. Comparisons of Z scores and biochemical markers between these two groups were subjected to

statistical analysis (Student's *t*-test; StatView-J 4.5). A *P*-value of less than 0.05 was considered statistically significant.

Results

Association of ALOX15 Gene Polymorphism With Bone Mineral Density

Among our 319 subjects, 46 were GG homozygotes, 155 were GA heterozygotes, and 118 were AA homozygotes. Allelic frequencies were 0.613 for the A allele and 0.387 for the G allele in this population. The allelic frequencies of this SNP in the present study were in Hardy-Weinberg equilibrium.

We compared the 273 subjects bearing at least one chromosome with the A allele (genotype GA + AA) and the 46 subjects having no A allele (GG) with respect to their Z scores for lumbar spine and total body BMD. Those with the A allele had significantly lower Z scores for lumbar spine BMD (-0.25 $\pm$ 1.34 versus 0.48 $\pm$ 1.70; p = 0.0014) (Fig. 1A) and total body BMD (0.25 $\pm$ 1.01 versus 0.62 $\pm$ 1.11; p = 0.048) (Fig. 1B). As shown in Table 1, the background and biochemical data did not significantly differ between these groups.

Discussion

Various regulating elements have been identified within the *ALOX15* 5'-flanking promoter/enhancer region, including a site for binding with Sp1 [25], AP1 [25], and GATA [26], as well as sites for methylation [27] and acetylation [28, 29] and a Stat6 response element [29], suggesting that 15-lipoxygenase expression is directly regulated through transcription regulation. In the present study, we observed a significant association between BMD and a G/A SNP at the –5299 site in the *ALOX15* 5'-flanking region. This is the first report to our knowledge that a common SNP in the *ALOX15* gene affects on BMD. One possible explanation for this effect is that this 5' -flanking region polymorphism may be involved in the newly defined transcriptional regulating element of the *ALOX15* promoter/enhancer. Alternatively, the 5'-flanking region polymorphism may have a linkage with another base of the *ALOX15* promoter/enhancer that may control transcription of the *ALOX15* gene. It is also possible that this SNP may be linked with mutation of the *ALOX15* exons or another unidentified gene adjacent to the *ALOX15* locus, which affect on the bone mass.

Although there are three lipoxygenases in humans, *ALOX15*, *ALOX15B*, and *ALOX12*, that correspond to 12/15-lipoxygenase in mice [23], we know little of their

roles in human bone metabolism. Our results suggest that the 15-lipoxygenase type1, the *ALOX15*, may have a specific function in the regulation of bone mass in human. It should be required to determine how signals from 15-lipoxygenase can be transduced to the regulation of the bone metabolism.

Three major cellular events are involved in senile osteoporosis; they are declining levels of osteogenesis, increasing numbers of apoptotic osteoblasts and osteocytes, and increasing levels of bone marrow adipogenesis [30-32]. The bone marrow adipogenesis that occurs with aging may be due to alterations in cell differentiation, in part by PPARγ activation [33-35] and increasing lipid oxidation [36]. Previous reports demonstrated that 12/15-lipoxygenases are involved in this system [17, 18, 37, 38], suggesting that 12/15-lipoxygenase may increase with aging in progenitor cells and activate adipogenesis. It has been also shown that 12/15-lipoxygenase is increased in Alzheimer's disease, which is the most common neurodegenerative disorder of the elderly [39]. Therefore, it is tempting to speculate that 12/15-lipoxygenase is increased associated with aging and senile osteoporosis. To test this hypothesis, measurement of 12/15-lipoxygenase activity and association study between BMD and the *ALOX15* gene SNP in older subjects would be desired.

In conclusion, our finding suggests that the *ALOX15* gene may be a genetic determinant of BMD in postmenopausal women. Examining the variation in the *ALOX15* gene will hopefully enable us to elucidate one of the mechanisms of involutional osteoporosis. Furthermore, the variation may be a potential genetic susceptibility factor that need to be further evaluated with regard to the risk of other diseases in which 15-lipoxygenase have been clearly implicated, including atherosclerosis [40], asthma [41], cancer [42] and glomerulonephritis [43].

Acknowledgments

This work was partly supported by grants from the Japanese Ministry of Health, Labor and Welfare and the Japanese Ministry of Education, Culture, Sports, Science and Technology. We thank Ms. E. Sekine, C. Onodera, and M. Kumasaka for expert technical assistances.

References

1. Kanis JA, Melton LJ 3rd, Christiansen C, Johnston CC, Khaltaev N (1994) The diagnosis of osteoporosis. J Bone Miner Res 9:1137-1141
2. Flicker L, Hopper JL, Rodgers L, Kaymakci B, Green RM, Wark JD (1995) Bone density determinants in elderly women: a twin study. J Bone Miner Res 10:1607-

1613

3. Young D, Hopper JL, Nowson CA, Green RM, Sherwin AJ, Kaymakci B, Smid M, Guest CS, Larkins RG, Wark JD (1995) Determinants of bone mass in 10 to 26 year old females: a twin study. J Bone Miner Res 10:558-567
4. Krall EA, Dawson-Hughes B (1993) Heritable and life-style determinants of bone mineral density. J Bone Miner Res 8:1-9
5. Gueguen R, Jouanny P, Guillemin F, Kuntz C, Pourel J, Siest G (1995) Segregation analysis and variance components analysis of bone mineral density in healthy families. J Bone Miner Res 10:2017-2022
6. Nelson DA, Kleerekoper M (1997) The search for the osteoporosis gene. J Clin Endocrinol Metab 82:989-990
7. Liu YZ, Liu YJ, Recker RR, Deng HW (2002) Molecular studies of identification of genes for osteoporosis: the 2002 update. J Endocrinol 177:147-196
8. Morrison NA, Qi JC, Tokita A, Kelly PJ, Crofts L, Nguyen TV, Sambrook PN, Eisman JA (1994) Prediction of bone density from vitamin D receptor alleles. Nature 367:284-287
9. Uitterlinden AG, Burger H, Huang Q, Yue F, McGuigan FE, Grant SF, Hofman A, van Leeuwen JP, Pols HA, Ralston SH (1998) Relation of alleles of the collagen type Ialpha1 gene to bone density and the risk of osteoporotic fractures in postmenopausal women. N Engl J Med 338:1016-1021
10. Ogawa S, Urano T, Hosoi T, Miyao M, Hoshino S, Fujita M, Shiraki M, Orimo H, Ouchi Y, Inoue S. (1999) Association of bone mineral density with a polymorphism of the peroxisome proliferator-activated receptor gamma gene: PPARgamma expression in osteoblasts. Biochem Biophys Res Commun 260:122-126.
11. Urano T, Shiraki M, Ezura Y, Fujita M, Sekine E, Hoshino S, Hosoi T, Orimo H, Emi M, Ouchi Y, Inoue S (2004) Association of a single-nucleotide polymorphism in low-density lipoprotein receptor-related protein 5 gene with bone mineral density. J Bone Miner Metab 22:341-345
12. Meunier P, Aaron J, Edouard C, Vignon G (1971) Osteoporosis and the replacement of cell populations of the marrow by adipose tissue. A quantitative study of 84 iliac bone biopsies. Clin Orthop 80:147-154
13. Burkhardt R, Kettner G, Bohm W, Schmidmeier M, Schlag R, Frisch B, Mallmann B, Eisenmenger W, Gilg T (1987) Changes in trabecular bone, hematopoiesis and bone marrow vessels in aplastic anemia, primary osteoporosis, and old age: a comparative histomorphometric study. Bone 8:157-164

14. Wronski TJ, Walsh CC, Ignaszewski LA (1986) Histologic evidence for osteopenia and increased bone turnover in ovariectomized rats. Bone 7:119-123
15. Miniare P, Meunier PJ, Edouard C, Bernard J, Courpron J, Bourret J (1974) Quantitative histological data on disuse osteoporosis. Calcif Tissue Res 17:57-73
16. Wang GW, Sweet D, Reger S, Thompson R (1977) Fat cell changes as a mechanism of avascular necrosis in the femoral head in cortisone-treated rabbits. J Bone Joint Surg 59A: 729-735.
17. Klein RF, Allard J, Avnur Z, Nikolcheva T, Rotstein D, Carlos AS, Shea M, Waters RV, Belknap JK, Peltz G, O rwoll ES (2004) Regulation of bone mass in mice by the lipoxygenase gene Alox15. Science 303:229-232
18. Huang JT, Welch JS, Ricote M, Binder CJ, Willson TM, Kelly C, Witztum JL, Funk CD, Conrad D, Glass CK (1999) Interleukin-4-dependent production of PPAR-gamma ligands in macrophages by 12/15-lipoxygenase. Nature 400:378-382
19. Kuhn H, Walther M, Kuban RJ, Wiesner R, Rathmann J, Kuhn H (2002) Prostaglandins Other Lipid Mediat 68-69:263-290
20. Nosjean O, Boutin JA (2002) Natural ligands of PPARgamma: are prostaglandin J(2) derivatives really playing the part? Cell Signal 14:573-583.
21. Lecka-Czernik B, Moerman EJ, Grant DF, Lehmann JM, Manolagas SC, Jilka RL (2002) Divergent effects of selective peroxisome proliferator-activated receptor-gamma 2 ligands on adipocyte versus osteoblast differentiation. Endocrinology 143:2376-2384
22. Khan E, Abu-Amer Y (2003) Activation of peroxisome proliferator-activated receptor-gamma inhibits differentiation of preosteoblasts. J Lab Clin Med 142:29-34
23. Krieg P, Marks F, Furstenberger G (2001) A gene cluster encoding human epidermis-type lipoxygenases at chromosome 17p13.1: cloning, physical mapping, and expression. Genomics 73:323-330
24. Asai T, Ohkubo T, Katsuya T, Higaki J, Fu Y, Fukuda M, Hozawa A, Matsubara M, Kitaoka H, Tsuji I, Araki T, Satoh H, Hisamichi S, Imai Y, Ogihara T (2001) Endothelin-1 gene variant associates with blood pressure in obese Japanese subjects: the Ohasama Study. Hypertension 38:1321-1324
25. Kelavkar U, Wang S, Montero A, Murtagh J, Shah K, Badr K (1998) Human 15-lipoxygenase gene promoter: analysis and identification of DNA binding sites for IL-13-induced regulatory factors in monocytes. Mol Biol Rep 25:173-182
26. Kamitani H, Kameda H, Kelavkar UP, Eling T (2000) A GATA binding site is involved in the regulation of 15-lipoxygenase-1 expression in human colorectal

carcinoma cell line, caco-2. FEBS Lett 467:341-734

27. Liu C, Xu D, Sjoberg J, Forsell P, Bjorkholm M, Claesson HE (2004) Transcriptional regulation of 15-lipoxygenase expression by promoter methylation. Exp Cell Res 297:61-67
28. Kamitani H, Taniura S, Ikawa H, Watanabe T, Kelavkar UP, Eling TE (2001) Expression of 15-lipoxygenase-1 is regulated by histone acetylation in human colorectal carcinoma. Carcinogenesis 22:187-191
29. Shankaranarayanan P, Chaitidis P, Kuhn H, Nigam S (2001) Acetylation by histone acetyltransferase CREB-binding protein/p300 of STAT6 is required for transcriptional activation of the 15-lipoxygenase-1 gene. J Biol Chem 276:42753-42760
30. Kirkland JL, Dobson DE (1997) Preadipocyte function and aging: links between age-related changes in cell dynamics and altered fat tissue function. J Am Geriatric Soc 45:959-967
31. Justesen J, Stenderup K, Ebbesen EN, Mosekilde, Steiniche T, Kassem M (2001) Adipocyte tissue volume in bone marrow is increased with aging and in patients with osteoporosis. Biogerontology 2:165-171
32. Chan GK, Duque G (2002) Age-related bone loss: old bone, new facts. Gerontology 48:62-71
33. Daiscro DD Jr, Vogel RL, Johnson TE, Witherup KM, Pitzenberger SM, Rutledge SJ, Prescott DJ, Rodan GA, Schmidt A (1998) High fatty acid content in rabbit serum is responsible for the differentiation of osteoblasts into adipocyte-like cells. J Bone Miner Res 13:96-106
34. Kirkland JL, Tchkonia T, Pirtskhalava T, Han J, Karagiannides I (2002) Adipogenesis and aging: does aging make fat go MAD? Exp Gerontol 37:757-767
35. Duque G, Macoritto M, Kremer R (2004) 1,25(OH)2D3 inhibits bone marrow adipogenesis in senescence accelerated mice (SAM-P/6) by decreasing the expression of peroxisome proliferator-activated receptor gamma 2 (PPARgamma2). Exp Gerontol 39:333-338
36. Lecka-Czernik B, Moerman EJ, Grant DF, Lehmann JM, Manolagas SC, Jilka RL (2002) Divergent effects of selective peroxisome proliferator-activated receptor-gamma 2 ligands on adipocyte versus osteoblast differentiation. Endocrinology 143:2376-2384
37. Kiefer CR, Snyder LM (2000) Oxidation and erythrocyte senescence. Curr Opin Hematol 7:113-116
38. Spiteller G (2001) Lipid peroxidation in aging and age-dependent diseases. Exp

Gerontology 36:1425-1457

39. Pratico D, Zhukareva V, Yao Y, Uryu K, Funk CD, Lawson JA, Trojanowski JQ, Lee VM (2004) 12/15-lipoxygenase is increased in Alzheimer's disease: possible involvement in brain oxidative stress. Am J Pathol 164:1655-1662
40. Harats D, Shaish A, George J, Mulkins M, Kurihara H, Levkovitz H, Sigal E (2000) Overexpression of 15-lipoxygenase in vascular endothelium accelerates early atherosclerosis in LDL receptor-deficient mice. Arterioscler Thromb Vasc Biol 20:2100-2105
41. Shannon VR, Chanez P, Bousquet J, Holtzman MJ (1993) Histochemical evidence for induction of arachidonate 15-lipoxygenase in airway disease. Am Rev Respir Dis 147:1024-1028
42. Shureiqi I, Chen D, Lee JJ, Yang P, Newman RA, Brenner DE, Lotan R, Fischer SM, Lippman SM (2000) 15-LOX-1: a novel molecular target of nonsteroidal anti-inflammatory drug-induced apoptosis in colorectal cancer cells. J Natl Cancer Inst 92:1136-1142
43. Montero A, Badr KF (2000) 15-Lipoxygenase in glomerular inflammation. Exp Nephrol 8:14-19

Figure legends

Figure 1. Z scores of lumbar spine and total body BMD in subject groups with each genotype of *ALOX15* gene polymorphism in the 5'-flanking region (-5229G/A). **A** Z scores for lumbar spine BMD are shown for genotype AA+ GA and genotype GG. Values are expressed as mean ± SE. Numbers of subjects are shown in parentheses. **B** Z scores for total body BMD are shown in the same manner as in **A**.

Table 1. Comparison of background, BMD and biochemical data between subjects bearing at least one A allele (AA + GA) and subjects with no A allele (GG) in the *ALOX15* gene 5'-flanking region (-5299G/A).

Items	Genotype (mean ± SD)		*P* value
	GG	GA+AA	
Number of subjects	46	273	
Age (years)	69.0 ± 8.9	66.3 ± 8.9	NS
Height (cm)	149.5 ± 6.9	150.3 ± 6.1	NS
Body weight (kg)	49.6 ± 8.6	50.3 ± 7.9	NS
Lumber spine BMD (Z score)	0.48 ± 1.70	-0.25 ± 1.37	0.0014
Total body BMD (Z score)	0.62 ± 1.12	0.25 ± 1.01	0.048
ALP (IU/L)	185.6 ± 63.9	193.4 ± 66.0	NS
I-OC (ng/mL)	8.2 ± 3.2	7.8 ± 3.6	NS
DPD (pmol/μmol of Cr)	7.0 ± 3.0	7.6 ± 2.7	NS
Intact PTH (pg/mL)	38.6 ± 20.0	35.2 ± 15.1	NS
Calcitonin (pg/mL)	16.6 ± 4.5	23.1 ± 11.4	NS
1,25 $(OH)_2D_3$ (pg/ mL)	33.0 ± 7.7	35.7 ± 11.8	NS
TC (mg/dL)	193.0 ± 45.0	199.4 ± 36.5	NS
TG (mg/dL)	142.5 ± 74.0	142.4 ± 81.8	NS
% fat	32.1 ± 6.6	31.9 ± 7.7	NS
BMI	22.1 ± 3.0	22.1 ± 3.1	NS

BMD, bone mineral density; ALP, alkaline phosphatase; I-OC, intact-osteocalcin; DPD, deoxypyridinoline; PTH, parathyroid hormone; TC, total cholesterol; TG, triglyceride; BMI, body mass index; NS, not significant. Statistical analysis was performed according to the method described in the text.

Fig. 1.

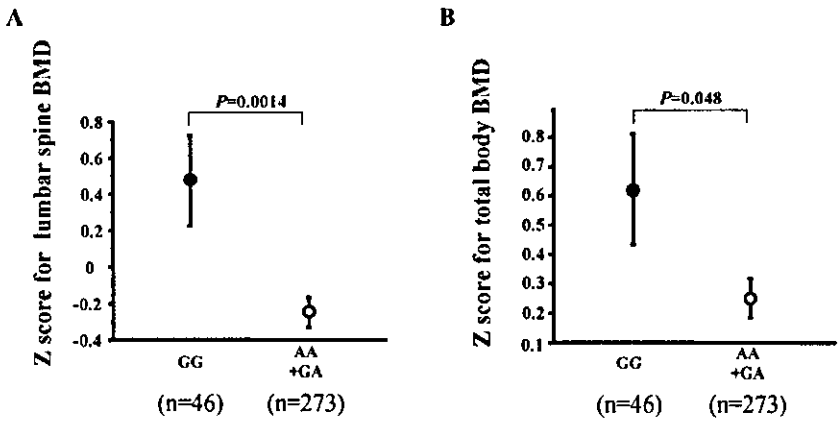
A
Z score for lumbar spine BMD
P=0.0014
0.8
0.6
0.4
0.2
0
-0.2
-0.4
GG
AA
+GA
(n=46)
(n=273)
B
Z score for total body BMD
P=0.048
0.8
0.7
0.6
0.5
0.4
0.3
0.2
0.1
GG
AA
+GA
(n=46)
(n=273)

Cancer Res (in press)

Estrogen Receptor-Binding Fragment-Associated Antigen 9 Is a Tumor-Promoting and Prognostic Factor for Renal Cell Carcinoma

Tetsuo Ogushi[1], Satoru Takahashi[1], Takumi Takeuchi[1], Tomohiko Urano[2], Kuniko Horie-Inoue[3], Jinpei Kumagai[1], Tadaichi Kitamura[1], Yasuyoshi Ouchi[2], Masami Muramatsu[3], Satoshi Inoue[2,3]

[1]Department of Urology and [2]Department of Geriatric Medicine, Faculty of Medicine, The University of Tokyo, 7-3-1 Hongo, Bunkyo-ku, Tokyo 113-8655, JAPAN. [3]Research Center for Genomic Medicine, Saitama Medical School, 1397-1 Yamane, Hidaka-shi, Saitama 350-1241, JAPAN

Financial Support: This work was supported by the Ministry of Health, Labor and Welfare Japan, the Ministry of Education, Culture, Sports, Science and Technology Japan.

Address correspondence to: Satoshi Inoue, Department of Geriatric Medicine, Graduate School of Medicine, The University of Tokyo, 7-3-1 Hongo, Bunkyo-ku, Tokyo 113-8655, JAPAN. Phone: +81-3-5800-8652; Fax: +81-3-5800-6530; E-mail: INOUE-GER@h.u-tokyo.ac.jp

Conflict of interests: none

Running Title: EBAG9 as a Tumor-Promoting Factor for Renal Cell Carcinoma

Key words: EBAG9, renal cell carcinoma, tumor growth, siRNA

Nonstandard abbreviations: estrogen receptor-binding fragment-associated antigen 9 (EBAG9); renal cell carcinoma (RCC)

ABSTRACT

The estrogen receptor-binding fragment-associated antigen 9 (EBAG9) has been identified as a primary estrogen-responsive gene in human breast cancer MCF7 cells. High expression of EBAG9 has been observed in invasive breast cancer and advanced prostate cancer, suggesting a tumor-promoting role of the protein in malignancies. Here we show that intratumoral administration of small interfering RNA (siRNA) against EBAG9 exerted overt regression of tumors following subcutaneous implantation of murine renal cell carcinoma (RCC) Renca cells. Overexpression of EBAG9 did not promote the proliferation of culture Renca cells, however, the inoculated Renca cells harboring EBAG9 (Renca-EBAG9) in BALB/c mice grew faster and developed larger tumors compared with Renca cells expressing vector alone (Renca-vector). After renal subcapsular implantation, Renca-EBAG9 tumors significantly enlarged compared with Renca-vector tumors in BALB/c mice, whereas both Renca-EBAG9 and Renca-vector tumors were developed with similar volumes in BALB/c nude mice. No apparent difference was observed in specific cytotoxic T cell responses against Renca-EBAG9 and Renca-vector cells, nonetheless, the number of infiltrating $CD8^+$ T lymphocytes was decreased in Renca-EBAG9 subcapsular tumors. Furthermore, immunohistochemical study of EBAG9 in 78 human RCC specimens showed that intense and diffuse cytoplasmic immunostaining was observed in 87% of the cases and positive EBAG9 immunoreactivity was closely correlated with poor prognosis of the patients. Multivariate analysis revealed that high EBAG9 expression was an independent prognostic predictor for disease-specific survival ($P = 0.0485$). Our results suggest that EBAG9 is a crucial regulator of tumor progression and a potential prognostic marker for RCC.

INTRODUCTION

Estrogen receptor-binding fragment associated gene 9, EBAG9, is an estrogen-responsive gene that we previously identified in MCF-7 human breast carcinoma cell line using a CpG-genomic binding site cloning method (1). EBAG9 protein, whose molecular size is 32 kDa by Western blot analysis, is expressed in estrogen target organs as well as several other tissues such as brain, liver, and kidney (2). The protein expression of EBAG9 is estrogen-inducible, as it has been shown in ovariectomized mice treated with 17β-estradiol administration (2). The physiological function of EBAG9 has not been well defined, yet the molecule may be implicated in cancer pathophysiology, with several lines of evidence of the protein expression in malignancies including breast (3), ovarian (4), prostate (5), and hepatocellular carcinomas (6). In prostate cancer (5), EBAG9 expression significantly correlated with advanced pathologic stages and high Gleason score ($P = 0.0305$ and $P < 0.0001$, respectively), suggesting the abundance of EBAG9 may relate to the progression of malignant tumors.

In the present study, we investigated whether EBAG9 expression is critical in tumor development of renal cell carcinoma (RCC). RCC that comprises the majority of kidney cancer is one of the ten most common malignancies in industrialized countries (7). The prognosis of patients with advanced RCC is poor, as 5-year survival rate is < 5% (8), and the treatment of metastatic RCC remains a difficult clinical challenge. Development of new and alternative modalities of diagnosis and therapy for RCC is a clinical requisite. We used murine syngeneic renal adenocarcinoma model of Renca cells in this study and investigated whether gene silencing or overexpression of EBAG9 influences Renca cell growth and/or *in vivo* tumorigenesis. Administration of small interfering RNA (siRNA) against EBAG9 regressed subcutaneous Renca tumors. The proliferation of culture Renca cells constitutively expressing EBAG9 was not basically different from control Renca cells, whereas EBAG9-expressing cells grew faster in BALB/c mice and developed larger tumors. The tumor-promoting effect of EBAG9 in Renca tumors may relate to the suppression of antitumor immunity, as intratumoral $CD8^+$ T lymphocytes were reduced in renal subcapsular Renca tumors. The tumorigenic relevance of EBAG9 in Renca models further extended to clinicopathological significance of the molecule in human RCC. EBAG9 immunoreactivity was closely correlated with poor prognosis of the patients and it was an independent prognostic predictor for disease-specific survival. Our findings demonstrate that EBAG9 is a tumor-promoting factor and a potential prognostic marker in RCC.

MATERIALS AND METHODS

Reagents. Rabbit anti-EBAG9 polyclonal antibody was generated against a fusion protein of glutathione-S-transferase and EBAG9 (2). Rabbit polyclonal anti-human CD3 antibody (DAKO Cytomation, Carpinteria, CA), rat anti-mouse CD4 (L3T4)(clone RM 4-5) and rat anti-mouse CD8a (Ly-2)(53-6.7) monoclonal antibodies (BD Pharmingen, San Diego, CA), and anti-β-actin monoclonal antibody (Sigma, St. Louis, MO) were commercially purchased. Human EBAG9 cDNA was cloned into a mammalian expression vector pcDNA3 (Invitrogen,

Carlsbad, CA).

Tumor Cells. Renca is a spontaneously arising murine renal cell carcinoma and was prepared as previously described (9, 10). Tumor cells were maintained in RPMI1640 containing 10% fetal calf serum and antibiotics.

Mice. BALB/c mice and BALB/c nu/nu mice (Nisseizai, Tokyo, Japan), which were syngeneic to Renca cells, were kept under specific-pathogen-free conditions and fed dry food and water. All mice used for experiments were male at the age of 5 weeks.

Patients and Tissue Preparation. We investigated 78 tissue samples of renal cell carcinoma obtained from patients (14 females and 64 males) who underwent radical or partial nephrectomy at Tokyo University Hospital between the years 1990 and 1995. Patient information was retrieved from the review of patient charts. Staging and grading of the tumors were performed according to the 1997 International Union Against Cancer TNM classification and WHO histopathological typing, respectively (11). The mean age of this population was 54 years old (26-76 years old) and the mean follow-up period was 60 months (2-78 months). For 32 patients with advanced tumors (pT2 or greater), adjuvant therapy was performed including immune therapy (n = 30), radiation (n = 5) and surgery for metastatic diseases in lung, colon, and pancreas (n = 8). During the follow-up period, 55 patients (70.5%) survived without evidence of disease, 8 cases (10.3%) presented with tumor recurrence, and 15 cases (19.2%) died of disease. None died of other diseases.

Western Blot Analysis. Cells were lysed in RIPA buffer [50 mM Tris-HCl, pH8.0, 200 mM NaCl, 20 mM NaF_2, 2 mM EGTA, 1 mM dithiothreitol, 2 mM sodium vanadate, 0.5% v/v Nonidet P-40 supplemented with a protease inhibitor cocktail Complete (Boehringer Manheim GmbH, Mennheim, Germany)] and proteins were resolved by 12.5% SDS-PAGE, transferred to polyvinylidene difluoride membranes. Membranes were probed with rabbit anti-EBAG9 antibody or anti-β-actin monoclonal antibody.

Tumor Regression by EBAG9 siRNA. Small interfering RNA (siRNA) duplex that targets EBAG9 was generated by Dharmacon (Lafayette, CO). The target sequence of EBAG9 siRNA was 5'- AAG AAG AUG CAG CCU GGC AAG -3'. Scramble II Duplex (Dharmacon) was used as a non-targeting control siRNA that does not possess homology with known gene targets in mammalian cells. The GC content of Scramble II Duplex was 57.9%, which was identical to that of EBAG9 siRNA.

To investigate *in vivo* silencing effect of EBAG9 siRNA in Renca tumors, intratumoral injection of siRNA duplexes was performed twice every week. Briefly, Renca cells (1×10^4 cells) were implanted in the flank of BALB/c mice. Tumor size measured weekly with a micrometer in two dimensions, and tumor volume was estimated according to the formula: $(\text{smallest diameter})^2 \times (\text{longest diameter})$. When the volumes of tumors reacheds 300 mm^3, siRNA duplexes (10 μg) were injected directly into tumors twice every week, along with 4 μl of GeneSilencer (Gene Therapy System, San Diego, CA) dissolved in 0.1 ml of Opti-MEM (Gibco BRL, Gaithersburg, MD). Mice were sacrified 4 weeks after treatment.

Generation of Renca Cells Stably Expressing EBAG9. Renca cells were transfected with an expression vector pcDNA3 including human EBAG9 cDNA or vector alone using

Lipofectamine (Gibco BRL, Gaithersburg, MD). G418-resistent cells were selected and several independent clones were isolated.

Reverse Transcription PCR. Total cellular RNA of Renca cells was extracted using ISOGEN reagent (NIPPON GENE, Tokyo, Japan) and first-stand cDNA was generated from 5 μg of total cellular RNA using a reverse transcriptase Omniscript RT™ (QIAGEN, Tokyo, Japan) and random hexamers. To validate the expression of exogenous human EBAG9, reverse transcription (RT) PCR was performed using specific primers for human EBAG9 (sense: 5'-GCTACACAAGATCTGCCTTT-3', antisense: 5'-CTTCTTCATTAGCCGTTGTG-3'). The amplification was performed for 35 cycles at 62°C for annealing, using AmpliGold Taq polymerase (Perkin-Elmer).

***In Vivo* Tumor Challenge.** For subcutaneous implantation, transfected Renca cells (1 x 10^4 cells/ mice) suspended in 0.1 ml of complete medium were injected in the flank of BALB/c mice. Tumor volume was calculated weekly. In survival analyses, Renca-bearing mice were followed up for 14 weeks after implantation.

For renal subcapcular implantation, tumors cells (1 x 10^4 cells/ mice) suspended in 0.1 ml of complete media were inoculated into the subcapsule of the left kidney of BALB/c wild-type and nude mice. Mice were sacrificed 25 days after implantation and tumors were exicised.

Cell Proliferation Assay. Cells were seeded at a density of 1-3 x 10^5 cells/dish into 10-cm dishes and hemocytometer counting was performed every two days. Doubling time during exponential growth was determined by a formula: [incubation time (h) x $\log_{10}2$]/ [$\log_{10}$(cell number at sampling period) - $\log_{10}$(plating cell number)](12).

Proliferation assays were performed using the 2-(2-methoxy-4-nitrophenyl)-3-(4-nitrophenyl)-5-(2,4-disulfophenyl)-2H tetrazolium monosodium salt (WST-8) reagent (Nacalai, Kyoto, Japan)(13). The assay is based on the conversion of the MTT-like tetrazolium salt WST-8 to a water-soluble formazan by metabolically active cells, provides a quantitative determination of viable cells. Cells were seeded in 96-well plates at an initial density of 625-5,000 cells/well. At one hour after inoculation, cells were transfected with either EBAG9 siRNA or Scramble II Duplex (100 ng/well) using GeneSilencer reagent (Gene Therapy Systems). Assays were performed on days 0, 2, and 4. For cells cultured up to day 4, medium was once exchanged on day 2. Spectrophotometric absorbance at 450 nm (for formazan dye) was measured with absorbance at 620 nm for reference.

Cytotoxicity Assay. Renca-EBAG9 or Renca-vector cells were used as target cells. Splenocytes of Renca-bearing BALB/c mice were stimulated for 5 days *in vitro* with irradiated Renca cells at a splenocyte: tumor cell ratio of 20:1 in the presence of 1,000 IU/ml interleukin-2, and used as effector CTLs. Target cells were incubated with effector CTLs at various E/T ratios in a final volume of 200 μl for 18 h at 37°C. Lactate dehydrogenase release from cells with a damaged membrane was examined using CytoTox-ONE Reagent (Promega, Madison, WI) and fluorescence was measured with an excitation wave length of 560 nm and an emission wave length of 590 nm. Experiments were performed in triplicate.

Immunohistochemistry. Immunohistochemical studies were performed using the streptavidin-biotin amplification method with horseradish peroxidase detection. Paraffin

sections of tumors were blocked in 0.3% H_2O_2 (30 min) and in 10% FCS (30 min), incubated overnight with specific antibodies against CD3, CD4, or CD8a for Renca tumors (1:20 dilution), or with purified rabbit anti-EBAG9 antibody for human RCC (1:40 dilution). Sections were incubated with biotinylated rabbit ani-rat IgG or anti-rabbit EnVison$^+$ reagent (Dako), developed by diaminobenzidine (Sigma) and counterstained with hematoxylin (Sigma). Negative controls were performed for each slide, using nonimmune IgG.

In Renca experiments, numbers of tumor infiltrating-lymphocytes (TILs) positive for CD3, CD4, or CD8 expression were microscopically examined in the high power field (HPF) of view at a magnification of 400X (14). BALB/c mouse spleen specimen was used as a positive control.

In RCC examination, immunoreactivity (IR) scores of EBAG9 expression were determined by two pathologists according to percentages of positive cells. Human breast cancer section (DAKO) was used as a positive control. Positivity was 0-4% for IR score 0 (negative), 5-24% for 1+, 25-49% for 2+, 50-100% for 3+. Sections that had $\geq 25\%$ positive cells but apparent lower intensity compared with positive controls were scored as IR score 1+. IR scores 1+, 2+, and 3+ were defined as positive staining. If IR scores were different between two pathologists, the average IR score was adopted. If several types of histology were included in one section, IR score of predominant histology was utilized.

Statistical Analyses. Comparisons between different groups of Renca samples were analyzed with non-parametrical Mann-Whitney U test. The associations between EBAG9 immunoreactivity and clinicopathological characteristics were evaluated by student-*t* test or Fisher's exact probability test. Disease-specific survival was computed by Kaplan-Meier method and the curves were compared by log-rank test. Multivariate analysis of prognostic factors was performed using Cox-proportional hazard regression model. Computations were done with the StatView 5.0J software (SAS Institute Inc., Cary, NC). All *P* values are two-sided and evaluated as significant if < 0.05.

RESULTS

Gene silencing of EBAG9 suppressed *in vivo* tumor growth of Renca cells. To determine the role of EBAG9 in tumor growth of renal cancer cells, we investigated the effects of synthesized siRNA duplexes targeting EBAG9 on subcutaneous tumor models of Renca cells implanted in syngeneic BALB/c mice. Intratumoral injection of EBAG9 siRNA reduced the protein levels of endogenous EBAG9 compared with the levels of EBAG9 in parental Renca cells or in the Renca tumor treated with control scrambled siRNA duplexes (Fig. 1A). Under the treatment of scrambled siRNA, subcutaneously implanted Renca cells developed prominent tumors, whereas the injection of EBAG9 siRNA suppressed tumor growth of Renca cells (Fig. 1B and 1C). After 4-week treatments, the volume of tumors with EBAG9 siRNA treatment was significantly smaller than that with scrambled siRNA ($3,854 \pm 665$ mm^3 *versus* $6,315 \pm 1,053$ mm^3, n = 5; $P = 0.0472$). We infer that tumor growth is modulated by EBAG9 expression, implicating EBAG9 as a tumor-promoting factor in renal carcinoma.

Generation of Renca cells stably expressing EBAG9. To explore whether constitutive EBAG9 expression influences tumor growth, we generated Renca cells stably expressing human EBAG9. We selected two Renca-EBAG9 cell clones #3 and #4 that express human EBAG9 mRNA as comfirmed by RT-PCR using human EBAG9 specific primers (Fig. 2A, top panel). The amounts of EBAG9 proteins in Renca-EBAG9 cells were ~2.0 fold increased compared with those in parental Renca cells and Renca-vector cell clones #1 and #2, that were transfected with pcDNA3 empty vector (Fig. 2A, bottom panel). In terms of cell growth rate, doubling time of culture Renca-EBAG9 cells was not significantly different from that of Renca-vector cells (Fig. 2B). Proliferation of Renca cells was further analyzed by a colorimetric MTT-like assay using a tetrazolium monosodium salt WST-8 that is converted to a water-soluble formazan by metabolically active cells (Fig. 2C). Neither EBAG9 overexpression nor RNA interference against EBAG9 did not significantly influence the growth of Renca cells. Moreover, EBAG9 overexpression did not influence the incorporation of BrdU in culture Renca cells (data not shown). The results suggest that stable expression of EBAG9 itself does not accelerate the proliferation of culture tumor cells.

EBAG9 promotes *in vivo* tumor growth of Renca cells. In spite of little difference of propagation abilities between Renca-EBAG9 cells and Renca-vector cells in culture, Renca-EBAG9 cells subcutaneously implanted into BALB/c mice developed more than 4-fold larger tumors compared with Renca-vector cells at 4 weeks after inoculation (Fig. 3A and 3B). Mean tumor volumes at 4 weeks were 1,712 ± 506 mm^3 for Renca-EBAG9 cell clones #3 and #4 *versus* 366 ±110 mm^3 for Renca-vector cell clones #1 and #2 ($P = 0.0055$, Fig. 3B).

In terms of prognosis of mice harboring Renca tumors, 23.5% of mice with Renca-vector cells (n = 17) survived on day 100 after tumor challenge whereas only 5.6% of mice with Renca-EBAG9 cells (n = 18) survived at the same period (Fig, 3C, $P = 0.0412$ by log-rank test). Systemic metastases, including tumor dissemination into peritoneum and distant metastases of lung and liver, were reasons for death in all deceased cases.

EBAG9 suppresses host immune surveillance. To determine whether aberrant EBAG9 expression in Renca cells affects the local immune responses in tumors, we implanted Renca-EBAG9 cells or Renca-vector cells under the renal capsule of BALB/c mice and immunodeficient BALB/c nude mice. Both Renca cell lines formed macroscopic tumors in all of the cancer-bearing hosts by Day 25 (Fig. 4A). In conventional BALB/c mice, Renca-EBAG9 tumors grew significantly larger compared with Renca-vector tumors (Fig. 4A and 4B). Mean volumes of tumors on Day 25 in BALB/c mice were 856 ± 162 mm^3 (n = 19) for Renca-EBAG9 clones #3 and #4 *versus* 149 ± 59 mm^3 (n = 18) for Renca-vector clones #1 and #2 (Fig. 4B, $P < 0.0001$). In immunodeficient BALB/c nude mice, both Renca-vector cells and Renca-EBAG9 cells developed extensive tumors compared with tumors in BALB/c mice and there was no significant difference in tumor volumes between Renca-vector cells and Renca-EBAG9 cells (Fig. 4A and 4B). Mean volumes of tumors on Day 25 in BALB/c nude mice were 2,215 ± 227 mm^3 (n = 18) for Renca-EBAG9 clones #3 and #4 versus 1,802 ± 240 mm^3 (n = 23) for Renca-vector clones #1 and #2 (Fig 4B, $P = 0.118$). These results may suggest that aberrant EBAG9 expression in Renca cells hampers a local primary immune response that retards the growth of

tumors, rather than potentiates the intrinsic tumorigenicity of the tumor cells.

To investigate whether the progression of Renca-EBAG9 tumors depends on a reduced sensitivity of the cells to tumor-specific CTLs, we performed cytotoxicity assays. Effector CTLs were derived from splenocytes of Renca-bearing BALB/c mice, after 5-day restimulation with Renca cells in the presence of interleukin-2. (Fig. 4C). Renca-EBAG9 cells and Renca-vector cells were equally lysed by tumor-specific CTLs, suggesting that EBAG9 expression itself does not affect the sensitivity of Renca cells to CTL lysis.

To assess whether EBAG9 modulates the subtype-specific reactivity of T lymphocytes against tumors, we examined the numbers of TILs in renal subcapsular Renca tumors developed in BALB/c mice (Fig. 4D). No significant differences in numbers of $CD3^+$ and $CD4^+$ T cells were observed between Renca-vector and Renca-EBAG9 tumors, whereas the number of $CD8^+$ T cells in Renca-EBAG9 tumors was significantly decreased compared with that in Renca-vector tumors ($P < 0.05$).

Expression of EBAG9 protein in human RCC tumors. The finding that EBAG9 modulated the growth of Renca tumors led us to the notion whether the molecule contributes to the progression of renal cell carcinoma in human tissues. EBAG9 expression was evaluated immunohistochemically in 78 RCC whole tissue specimens including normal lesions. In non-carcinomatous lesions, a weak and scattered immunostaining of EBAG9 was observed in the cytoplasm of the mesangial cells (Fig. 5A) as well as on the luminal surface of the renal tubular cells (data not shown). The levels of EBAG9 expression in normal renal tissues corresponded to IR score 0. In RCC tumors, 10 of 78 cases (13%) had negative immunoreactivity of EBAG9, whereas 68 of cases (87%) showed EBAG9 positivity. In regard to EBAG9-positive RCC tumors, the cancer cells generally retain intense and diffuse staining patterns in the cytoplasm or on the membrane (Fig. 5B, C, and D). The levels of EBAG9-positivity were IR score 1+ for 18 RCC tumors (23%), 2+ for 31 tumors (40%), and 3+ for 19 tumors (24%). With respect to RCC histology, clear cell tumors displayed an intense membrane staining as well as a diffuse cytoplasmic staining of EBAG9 (Fig 5B, IR score 2+). Sarcomatoid tumors showed an intense and frequent cytoplasmic immunoreactivity (Fig 5C, IR scores 3+). Lung metastatic tumors showed the highest EBAG9 staining, predominantly in the cytoplasm (Fig 5D, IR score 3+).

A significant association between EBAG9 immunoreactivity and clinicopathological parameters was observed in RCC patients (Supplementary Table 1). EBAG9 positivity (IR score >1+) was significantly correlated with advanced pathological tumor stages, positivity of vascular infiltration, and non-clear cell histology ($P = 0.0017$, $P = 0.0109$, and $P = 0.0126$, respectively).

In Kaplan-Meier analysis of the RCC patients, those in which the tumor had high EBAG9 immunoreactivity (IR score 3+) showed a shorter disease-specific survival (Fig. 6) compared with patients showing low or negative EBAG9 immunoreactivity (IR score 0–2+). The 5-year disease-specific survival in cases with EBAG9 IR score 3+ was 55% whereas 91.2% of patients with low or negative EBAG9 immunoreactivity were alive during the same period.

In univariate Cox proportional hazards analysis for 5-year disease-specific survival, established prognostic factors including infiltration, pathological stage, and metastatic status are

the most significant univariate parameters of survival (Supplementary Table 2; $P < 0.0001$ for all). Lower EBAG9 immunoreactivity as well as negativity of lymph node status or vascular infiltraion are also involved in significant univariate survival predictors ($P = 0.0007$, 0.0002, and 0.0003, respectively). In multivariate Cox proportional hazards analysis, negative metastatic status is the most significant predictor of survival (Supplementary Table 3; $P < 0.001$; relative risk, 42.53) Notably, high EBAG9 immunoreactivity is associated with disease-specific death in multivariate analysis ($P = 0.0485$; relative risk, 5.09). These results indicate that high immunoreactivity of EBAG9 is a potential poor prognostic parameter in RCC patients.

DISCUSSION

The present study shows the first evidence regarding a tumor-promoting role of EBAG9 *in vivo*. We showed that Renca tumors overexpressing EBAG9 had a much aggressive phenotype with poorer prognosis as compared to Renca tumors expressing empty vector, although the effects of EBAG9 on culture cell proliferation was relatively minimal. EBAG9 immunoreactivity was detected in most of human RCC samples and high amounts of EBAG9 protein may associate with poor prognosis of the patients. Our findings suggest that EBAG9 is a tumor-promoting factor in RCC yet does not function as an essential oncogene by itself. The present results lead us to the notion that EBAG9 potentiates tumor growth by altering tumor microenvironment.

Decreased local immune responses may one of the critical machanisms that change tumor microenvironment. In antitumor immunity, T lymphocyte-mediated immune surveillance is thought to be a principal host defense mechanism (15). Although tumors such as RCC are immunogenic and could be targeted by tumor-specific CTL or natural killer cells, antitumor immune reactions are not completely effective to reject tumor cells so that tumors continue to grow progressively (16). In our cytotoxicity assay, there was no significant difference of CTL lysis between Renca-EBAG9 and Renca-vector cells, suggesting that overexpression of EBAG9 may not particularly alter the presentation of tumor-associated antigens or the levels of MHC class I molecule expression. In TIL assay, however, $CD8^+$ T cells seemed to be specifically reduced by aberrant EBAG9 expression. We suspect that generation of immunosuppressive factors or apoptosis activation may result in the reduction of $CD8^+$ TIL, leading to hamper antitumor immunity.

The alteration in cell surface glycosylation could be implicated in the modulation of tumor microenvironments (17, 18). It has been recently shown that tumor-associated ganglioside expression in human RCC cells suppresses nuclear factor-κB activation in T cells and mediates T-cell apoptosis (19, 20). RCC display increased levels of gangliosides including GM2, GM1, and GD1a (21) as well as several disialogangliosides (22), which may inhibit the function of antigen presenting cells (23) or modulate tumor vascularization (24). It has been recently shown that tumor-associated *O*-linked glycan antigens Tn and TF were expressed in transfected cells expressing RCAS1 (receptor-binding cancer antigen expressed on SiSo cells)(25), whose cDNA has been found to be a homolog of EBAG9 (26).

Another possible explanation is that EBAG9 may stimulate angiogenesis by up-regulating growth factors or cytokines. There are literatures that vascular endothelial growth factor (VEGF) could be involved in RCC tumor progression. Mutations of the von Hippel-Lindau tumor suppressor gene, which are often observed in hereditary RCC and sporadic clear-cell RCC, result in overproduction of VEGF through a mechanism involving hypoxia-inducible factor α (27, 28). It has been recently shown that VEGF interferes with the development of T cells at pathologically relevant concentrations *in vivo* (29), thus the growth factor may contribute to tumor-associated immune deficiencies.

It has been generally accepted that tumor cells may escape from immune surveillance by expressing the EBAG9 homolog RCAS1, which targets RCAS1 receptor-expressing immune cells and induces apoptosis (26). Nakashima *et al.* identified the RCAS1 cDNA through expression cloning using the 22-1-1 monoclonal antibody that they originally generated (30). Engelsberg *et al.* recently showed, however, that the 22-1-1 epitope was distinct from the products encoded by RCAS1 cDNA, because RCAS1 protein was not recognized by the 22-1-1 antibody whereas the 22-1-1 antibody recognized the tumor-associated *O*-linked glycan antigens (25). They showed that their raised polyclonal antibody recognized a ~35 kDa protein, consistent with the immunoblotting results using our polyclonal antibody. On the contrary, putative RCAS1 protein recognized by the 22-1-1 antibody was identified as a ~80-kDa membrane molecule expressed on human uterine cancer cells (26, 30). Although there are a number of publications concerning RCAS1 in cancers from the point of view as the 22-1-1 antigen, we consider that a pathophysiological role of EBAG9 in tumor immunology needs to be properly evaluated. The present manuscript may provide new insights into an EBAG9-mediated *in vivo* function in cancer progression.

We have previously reported that the immunoreactivity of EBAG9 was mainly observed in the cytoplasm of normal epithelial cells with a granular staining pattern, or particularly in perinuclear regions (3, 5). In carcinoma tissues, an intense staining of the cell surface could be also observed such as in prostate cancer or hepatocellular carcinoma. The expression of RCAS1 immunoreactivity recognized by antibodies against recombinant RCAS1 was localized to perinuclear structures, suggesting that the protein is predominantly distributed in the Golgi system (25). Given that EBAG9 is a Golgi-predominant protein that could be trafficking from the perinuclear regions to the cell surface membrane, it is likely that EBAG9 immunoreactivity could be observed in both cytoplasm and cell surface of carcerous tissues with the abundant expression of EBAG9. Notably, EBAG9 immunoreactivity in RCC with advanced stages such as sarcomatoid or metastatic tumors was cytoplasmic-predominant (Fig. 5C and 5D). Further studies using confocal or electron microscopic examination may elucidate the dynamic distribution of EBAG9.

As we showed that there are several types of cancer that intensely express EBAG9 and the expression levels of EBAG9 may relate to advanced tumor grades (3-6), it is likely that the tumor-promoting effect of EBAG9 is a general event in malignancies regardless of their estrogen dependency. We also observed the lack of association between sex and EBAG9 expression in human RCC in our clinicopathological study (Supplementary Table 1). Thus,